



OPEN

Age and interpulse interval relation from newborn to adult sperm whale (*Physeter macrocephalus*) off Mauritius

Maxence Ferrari^{1,2}✉, Marie Trinh¹, François Sarano^{2,3}✉, Véronique Sarano^{2,3}✉, Pascale Giraudet^{1,2}✉, Axel Preud'homme^{2,4}, René Heuzey^{2,4} & Hervé Glotin^{1,2}✉

Sperm whales (*Physeter macrocephalus*) have been studied for decades, but the development of their clicks during the animal growth is not yet well known. The click they emit during socialization and echolocation contains information about the length of their acoustic organs and, therefore the length of the body through the interpulse interval (IPI). This paper provides the first IPI/age relationship for juvenile male and female sperm whales (*Physeter macrocephalus*) based on field recordings of individuals whose age is largely known. Across 9 years, audiovisual recordings of a Mauritian sperm whale social unit were carried out. Adult female and juvenile sperm whales were identified and aged. The dataset made from those recordings is publicly available. The interpulse interval was measured for individuals whose ages ranged from 7 days to around 38 years. The growth of the acoustic organ of juveniles showed an early inter-individual variability as well as sexual dimorphism. Usual growth models were also fitted, predicting a mean IPI_{∞} of 3.5 ms for adults and a physical maturity reached at around 30 years old. The use of passive acoustic monitoring (PAM) is one of the main tools used to study sperm whales. This IPI-age relationship may aid demographic studies on sperm whales by enabling PAM to assess the ages of recorded sperm whales.

The sperm whale *Physeter macrocephalus* (Linnaeus 1758) is the largest representative of the odontocetes. This species is spatially distributed worldwide¹, and it presents strong sexual segregation and dimorphism. Adult females and their offspring live in social groups in tropical waters, stay all their life within their natal group, and display strong philopatry to their birthplace. On the contrary, males attaining sexual maturity leave their natal social group and spend their lives traveling between high latitudes (feeding grounds) and low latitudes where they visit female social groups for mating and socializing, with no observation made of a male sperm whale visiting their natal group². The sexual dimorphism is strongly marked: adult males are up to one-and-a-half times the length of adult females (mean 16 m, 45 tons, and 11 m, 15 tons)^{1,2}. In this paper, adults designate individuals who have reached physical maturity (having reached the end of growth), and juveniles designate nonadult individuals. Sperm whales have the largest brains in the animal kingdom at up to 8 kg. Large brains have been linked to more complex social interaction in mammals³. Sperm whales communicate using clicks^{4,5}, but also use their acoustic apparatus to produce high intensity clicks for echolocation, which might have also been a selecting factor in this large encephalization^{6,7}. Their hypertrophied nose, which contains their acoustic organs, measures up to one-third of the total body length^{1,2,8}, also demonstrates the importance of acoustic in sperm whales.

Sperm whales emit clicks, that are classified by their pattern of emission¹⁰: coda clicks¹¹, slow clicks, echolocation clicks, and buzz clicks¹². They seldom emit other kinds of sounds named trumpets and meows. A click is composed of regularly spaced pulses produced between 0.2 kHz and 25 kHz^{5,13–15}. According to the bent horn theory^{15,16}, a first pulse bounces back and forth inside the acoustic organs of sperm whales, losing part of its energy at each cycle (Fig. 1). Several pulses, named P_n , can therefore be recorded in each click, with n being the number of the pulse starting from 0. In codas, the energy decay of each pulse is smaller than in echolocation clicks. Thus, more pulses can be observed in coda clicks than in echolocation clicks. In far field recording of clicks,

¹Université de Toulon, Aix Marseille Université, CNRS, LIS, DYNI, Toulon, France. ²CIAN, International Center of AI for Natural Acoustics, Univ. Toulon <https://cian.lis-lab.fr>. ³Longitude 181, 12 r. de La Fontaine, 26000 Valence, France. ⁴Indian Ocean Marine Life Foundation, 44, La bourdonnais Street, Port Louis, Mauritius. ✉email: maxence.ferrari@gmail.com; saranofrancois@gmail.com; veronique.sarano@longitude181.org; pascale.giraudet@univ-tln.fr; glotin@univ-tln.fr

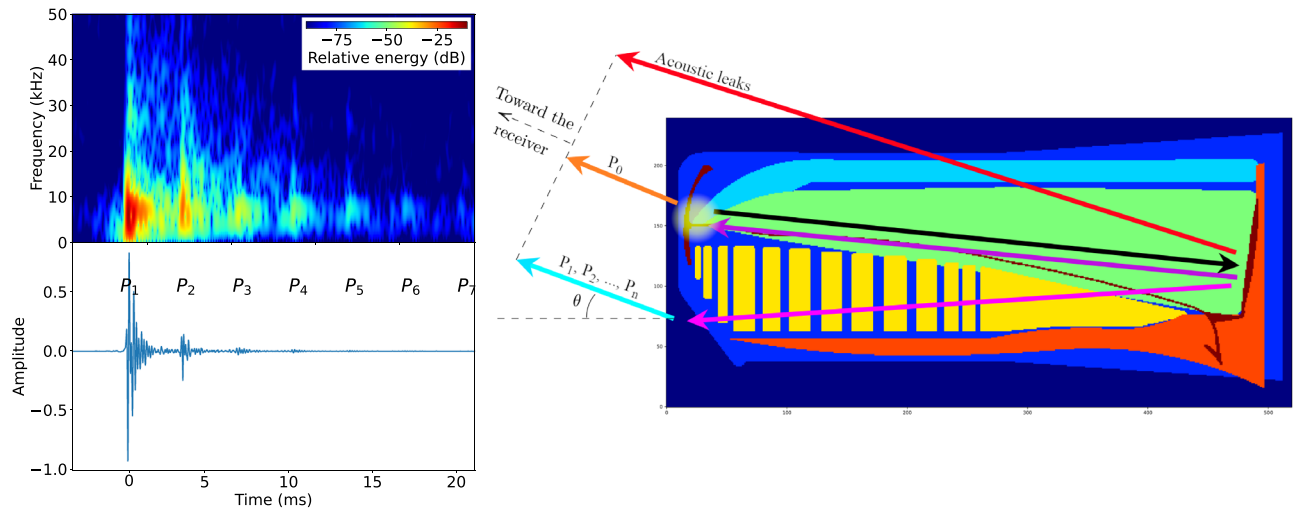


Figure 1. Left: A coda click from Tache blanche from 2018, with an IPI of 3.29 ms. Pulses from P_1 to P_7 can be seen. P_0 is not present, as it was recorded from behind. Right: Pulse path in the head of the sperm whale in the leaky bent horn model. Pulse is emitted at the monkey lips, indicated by the yellow spot (enlarged for visibility). P_0 goes straight into the water (from Ferrari⁹).

n can be reduced to 2 or 1. The regular time interval between these pulses is called the inter-pulse interval (IPI) and is directly linked to the size of the animal's head^{10,12,17–19}. The first pulse P_0 differs from the other pulses as it does not take the same acoustic path. While the time interval between P_0 and P_1 will not be exactly as long as the intervals between other P_n and P_{n+1} , it will have a similar value as it changes with the orientation of the animal compared to the recording device²⁰. The bent horn theory can also include other acoustic leaks, such as the red path in Fig. 1. In the context of sperm whales, acoustic leaks designate any energy that leaves the nose of the sperm whale following another path than either the P_0 's one or the P_n 's one. The interval between P_n and P_{n+1} is referred to as the nominal IPI as it does not vary no matter the receiver position. As the IPI is linked to the size of the sperm whale, it could be used to study the growth of sperm whales.

For other smaller cetacean species, growth has been studied using animals in captivity, allowing a precise knowledge of the age of each animal, and precise measurements of their body throughout their life, at the cost of the bias that captivity might bring. Since sperm whales cannot be kept in captivity, studies were mostly done on catches from whaling^{21–24}, and thus almost only contains animals above 7 m. More recently, another study was done on three mass strandings on the north and west coasts of Tasmania²⁵, but with only 6 individuals out of 86 under 8 m. The absence of information on those studied whales also means that the dates of birth were unknown. To estimate the ages of the measured specimens, the scientists used two methods. The first one used in all studies is based on the number of dentinal growth layers^{26,27}. Authors previously disagreed on the exact growth rate, with the rate taken as either one or two layers per year, with the latter seeming to be very unlikely^{22,24}. Even with the now agreed upon one layer per year²⁸, the number of layers for one animal will vary between each tooth²⁹, but this error source was not taken into account by the previous studies. The second method is based on the ovulation rate since in sperm whales the ovarian corpora stay in the ovaries. The mean ovulation rate was measured to be around 0.59 per year, but the rate seems to be decreasing after 12 ovulations²².

At birth, sperm whales range between 3.5 m and 4.5 m^{21,23,30}, with no presence of sexual dimorphism in terms of size³⁰. During growth, one aspect of sexual dimorphism is that males have another period of fast growth after the start of puberty^{22,24}. The ratio between the length at the start of puberty and the fully grown length seems to be a constant in all whales³¹. This ratio for sperm whales is said to be 72.7% by Berzin²¹ and also fits the data of Best²². It is possible that after reaching their maximum size, sperm whales might slowly shrink^{21,27}.

Previous studies have used combined age and length data to understand the growth rate of sperm whales. Almost all papers have hand-drawn the curve to fit their data. For Best²², the justification for not fitting a model is the presence of an inflection point in the growth curve of males. This inflection point is due to the second period of fast growth, which is not included in models such as the Gompertz³² and the Von Bertalanffy³³ models. Only two previous studies fitted those mathematical models^{25,34}. These curves can be seen in Fig. 2.

The equations of the fitted models are:

$$L(t) = L_0 \exp^{a(1 - \exp(-\alpha t))}, \quad (1)$$

$$L(t) = L_\infty \left(1 - \exp^{-a(t-t_0)} \right). \quad (2)$$

Eq. (1) is the Gompertz model where L_0 is the length at birth and Eq. (2) is the Von Bertalanffy model where L_∞ is the asymptote of the model when t goes toward ∞ (which can be thought of as the length at the end of the growth) and t_0 is the time at which the length is 0. In these models, a and α correspond to exponential growth parameters. Both models were fitted to the hand-drawn curves, and are reported in Table 1 along with the parameters of

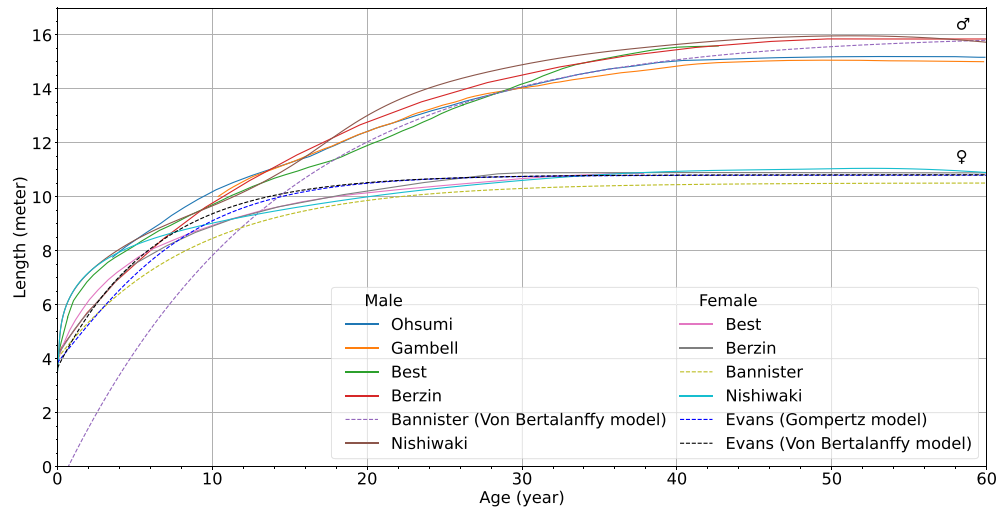


Figure 2. Growth curves of sperm whale from previous studies. All of the curves are redrawn from their original paper (full line), except for the curves from Bannister³⁴ and Evans et al.²⁵ which use their mathematical models (dotted line).

References	Gompertz			Von Bertalanffy		
	L_0	a	α	L_∞	a	t_0
Male						
Ohsumi ²⁴	6.522	0.8782	0.06742	15.94	0.05315	- 8.891
Gambell ²³	5.676	0.9965	0.07911	15.48	0.06782	- 4.568
Best ²²	6.021	1.0620	0.05462	19.06	0.03287	- 11.06
Berzin ²¹	3.586	1.4660	0.11550	15.94	0.07498	- 3.207
Bannister ³⁴	1.385	2.4140	0.11670	16.03	0.07200	+ 0.697
Nishiwaki et al. ²⁷	3.853	1.4080	0.10860	15.96	0.07761	- 3.255
Female						
Best ²²	3.216	1.1580	0.33200	10.37	0.22720	- 1.653
Berzin ²¹	3.287	1.1590	0.26460	10.66	0.17270	- 2.252
Bannister ³⁴	4.324	0.8852	0.14040	10.52	0.11500	- 4.177
Nishiwaki et al. ²⁷	3.422	1.1090	0.66290	10.51	0.33360	- 1.221
Evans et al. ²⁵	3.858*	1.0300	0.18000	10.82	0.16000	- 2.580 ◊

Table 1. Parameters for models in the literature. Bold: parameters fitted from the hand-drawn curves by using each pixel as a data point. Normal: parameters are given in the paper. * We fixed the parameters with $L_0 = \frac{L_\infty}{\exp a}$. ◊ The sign was changed from + to -. Both corrections to Evans et al.²⁵ were done because the parameters given in their paper do not match their results. The corrections we propose both fit their results and are obtained for the reported parameters suggesting they are the parameters they obtain when fitting their model.

models already given in Bannister³⁴ and Evans et al.²⁵. The parameters given in Evans et al.2004²⁵ do not match its figure but can be easily corrected as shown in Table 1.

The growth of sperm whales can also be observed acoustically³⁵. The spermaceti organ size is correlated to the size of the sperm whale²⁷. Since the duration of the IPI is linked to the size of the spermaceti organ, the sperm whale length can be extrapolated from the IPI. From this relation, multiple articles provided equations for this correlation. All those proposals differ as they investigate different groups (e.g. 15 m males, females), different locations, and sometimes only used a small number of individuals (e.g. 5, 11, 12^{36,37}). They are not suitable for juvenile sperm whales as they extrapolate to sizes above 7 m for small IPI (1.5 ms), when sperm whales are born at around 4 m^{25,27,30}. To our knowledge, IPI emitted for very young juveniles as only been reported by Tønnesen et al.³⁸ showing the need for more insights on clicks emitted by sperm whales during their first years. Thus, current formulas overestimate the size of juvenile sperm whales. Inversely, if these equations are inverted to predict an IPI from a length instead, they predict an IPI with a negative value for 4 m. The formulas we retained for this paper are:

$$L = 4.833 + 1.453 \text{ IPI} - 0.001 \text{ IPI}^2, \quad (3)$$

$$L = 5.736 + 1.258 \text{ IPI}, \quad (4)$$

$$L = 0.76 + 2.32 \text{ IPI} - 0.126 \text{ IPI}^2. \quad (5)$$

Eq. (3) was based on 11 sperm whales from Sri Lanka and the Azores, smaller than 12 m³⁶, while Eq. (4) was based on 33 New Zealand sperm whales larger than 12 m³⁷. Finally, we provide Eq. (5), a corrected version of the equation given by Møhl et al.³⁹. As noted by Gordon³⁶, this equation was based on a speed of sound in the spermaceti organ that was twice as fast. Hence, the correction simply replaces *IPI* by $\frac{\text{IPI}}{2}$ in the original equation. An alternative correction could use another speed of sound based on more recent papers^{40,41}. It was not attempted here as it was out of the scope of this paper.

The focus of this study is to measure the IPI's development during growth while considering sexual dimorphism. The study is based on the recording of the same identified individuals whose date of birth is known for many of them, and who belong to the same social unit over several consecutive years. This study is key to assess the development of the sperm whale acoustic organs and opens perspectives in large population acoustical studies.

Results

This study produced two main results. The first being the acoustic development of sperm whale clicks from a whole Mauritian clan (Irene's clan) over 9 years. All individuals were recorded in Mauritius (Indian Ocean). They were previously identified and, for many of them, their date of birth is known^{42,43}. This is the first IPI-age relation for juvenile male and female sperm whales based on field recordings of 26 individuals, 12 of which (8 juvenile males, 4 juvenile females) whose age is known (see Supplementary Material S1). The second main result is the fitting of mathematical models of development of the IPI.

Dataset

The dataset was created from videos where either a single sperm whale emitted clicks toward the audiovisual recorder, or when two sperm whales of a dyad were emitting codas. Most of the on-axis emitted clicks were social creaks, and other off-axis clicks were mainly codas. Slow clicks from male sperm whales were not used. Recordings were taken between 2013 and 2022 with a lack of chosen data in 2014 (Table 2) and a lack of data in 2021 due to Covid19 lockdown. The total length of the dataset is 2h 46min 3sec for a total number of 114 videos. Recordings with no evidence of IPI were not taken into account.

Sperm whale IPI

From acoustic data collected over 9 years in the same Irène's clan, we measured the IPI of 26 individuals aged from 7 days old to about 38 years old⁴². The outcome of this annotation effort is illustrated in Fig. 3.

Sexual dimorphism could be said to appear around 7 years old for Tache blanche and Elio as they have an IPI large enough to be outside of the 95% prediction interval of the female of that age (Fig. 4). We have noticed that the teeth are also visible at 7 years old for all juveniles and could indicate the beginning of puberty. For them, this dimorphism is clearly marked as early as 4 years old compared to Zoé. For both of them, the growth is similar, which is likely since they are half-brothers⁴³. This dimorphism is however not only due to sexual dimorphism (which might play no part at all) but also inter-individual dimorphism. Indeed, the IPI growth curve of one juvenile male (Roméo) is similar to the one of the juvenile female Zoé. Although Zoé is nine months younger than Roméo, they have similar body lengths when observed together. The future study of individuals such as Daren will show if Roméo is really small or if Eliot and Tache blanche that are tall. Similarly, a female juvenile can emit IPI as spaced as the larger male juvenile at the same young age. For example, Miss Tautou whose IPI of 2.51 ms is comparable to the one of Arthur, both at 3.1 years old. These two data points overlap in Fig. 3. It is in accordance with the lack of sexual dimorphism near birth and shows that the individual variability is large

Year	Number of videos	Video materials	Acoustic materials	Total length (min, sec)
2013	1	GoPro Hero 3	GoPro	3min 31sec
2015	7	GoPro Hero 3, Sony F55	GoPro	14min 15sec
2016	20	GoPro Hero 3, GoPro Hero 4, Sony F55	GoPro	27min 56sec
2017	24	GoPro Hero 3, GoPro Hero 4, Sony F55	JASON	25min 05sec
2018	36	GoPro Hero 3, GoPro Hero 8, Sony F55	JASON	24min 20sec
2019	25	GoPro Hero 7, Sony F55	JASON	53min 22sec
2020	10	GoPro Hero 8, Sony F55	GoPro	11min 47sec
2022	5	GoPro Hero 8, Sony F55	GoPro	5min 45sec

Table 2. Number of videos and recording acoustic materials used from 2013 to 2022. Blank cell indicated that no specific acoustic recording device was present this year, and that audio was only extracted from the videos.

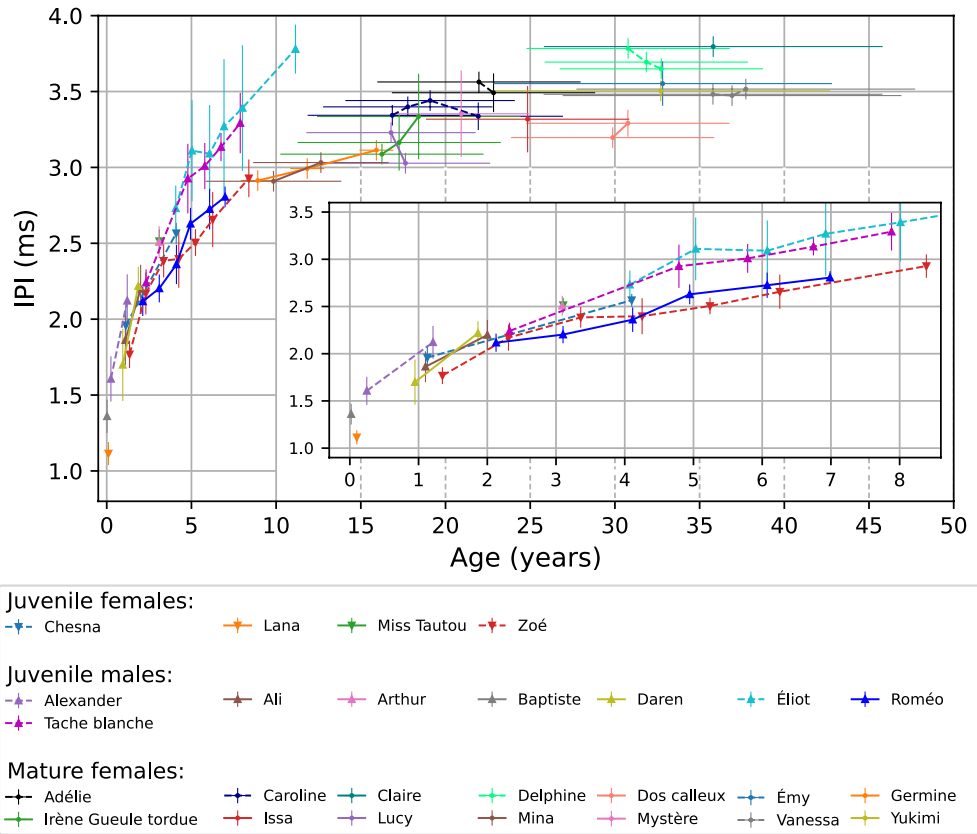


Figure 3. IPI-age relation linked to the growth of the acoustic organ of adult female and juvenile sperm whales, with a zoom on juvenile. The vertical bars are the standard deviations for the corresponding points. The horizontal bar is the standard deviation for the age and is only given for mature females for clarity. Dashed curves correspond to individuals belonging to Vanessa’s subgroup.

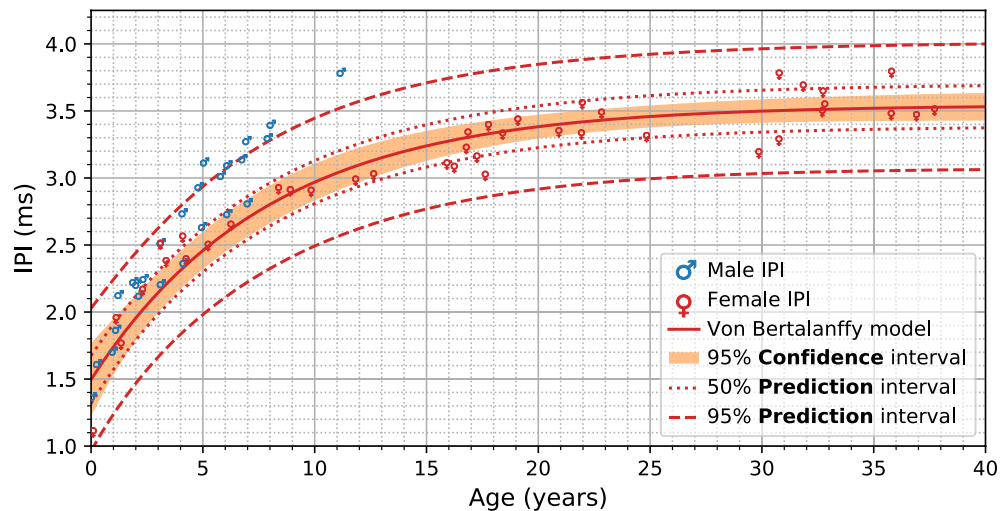


Figure 4. The Von Bertalanffy model fitted on the female sperm whales (Irène’s clan, Mauritius). The confidence interval is the interval in which the model could be due to the uncertainty of the parameters. The n% prediction interval is the interval in which n% of the population is present.

enough that, at the same age, the male and female populations cannot be distinguished by IPI alone. Nevertheless, starting between 5 and 7 years old (Fig. 4), the increased growth of males seems to be large enough such that their IPI can be distinguished from the one of a similarly aged female.

Regression model of the growth of sperm whales

From the collected data, we fitted the Gompertz (1) and Von Bertalanffy (2) growth model. The Von Bertalanffy fitted model is illustrated in Fig. 4, and the parameters are given in Table 3. Since we only have adult data for females, only a female model is plotted. The males' fitted parameters are still reported for completeness. The Gompertz model for females is not plotted in Fig. 4 because of its similarity to the Von Bertalanffy model would only hinder the figure's readability.

Concerning parameters that are linked to the end of the growth curve, the standard deviation is much higher for males than females, as expected by the lack of adult males. Note that if we remove Roméo from the data before fitting the male models, the average 95% confidence interval width is only 0.8 ms, with the largest error between the fitted curves and a data point being 0.12 ms, and tends to IPI_{∞} (IPI at the end of growth) that are even lower. Since the data is mostly composed of the half-brothers Tache blanche and Éliot after 3 years old, this is most likely due to the overfitting of these two individuals, and would not be representative of the general trend. Hence, we chose to not include the "males without Roméo"s results. The time $t_{72.7}$ at which Berzin²¹ said the female sperm whales reach their puberty is around 6 years old for both models. The age of physical maturity which ranges from 28 to 45 years old depending on the authors^{21–23,27,44} corresponds to our findings of the t_{99} of 30 years old where the female sperm whale has achieved 99% of its growth. Using Eqs. (3) and (4) for IPI_{∞} gives a final female size of 9.95 m and 10.18 m respectively.

The example of Roméo and the two half-brothers showed that inter-individual dimorphism can be significant even before the end of the growth. To account for this variability, the prediction interval was evaluated (only reported here for female). The width of the 95% prediction intervals starts from around 1.1 ms and stays constant at around 0.95 ms after 5 years. It is only 0.32 ms for the 50% prediction interval. Converting to length, the 95% prediction intervals become [9.26 m, 10.64 m] for Eq. (3) and [9.58 m, 10.77 m] for Eq. (4) respectively, meaning that most of the female adult sperm whale population have length that fit inside a range of 1.3 m. By combining the age-length models from the bibliography and our age-IPI models, a new IPI-age equation could be derived. However, sources of errors such as the large IPI variability for an age or the imprecision of growth models for juvenile sperm whales would lead to an incorrect equation. Thus, the equation $L = -4.634 + 6.345 IPI - 0.553 IPI^2$ derive from the Von Bertalanffy model from Evans et al.²⁵ and our Von Bertalanffy model is just given as an indication.

Discussion

Although a small number of individual sperm whales were recorded, this study gives the first IPI-age relation for juvenile females and males, based on individuals whose age is precisely known.

While adult males were present during the period of this study, we chose to not integrate them. The main reason was that the only type of click that visible males emitted during our recordings were slow clicks (also known as clangs) and we were unable to conclude on a coherent IPI value for those clicks. To our knowledge, there is no IPI study based on slow clicks. Echolocation clicks from adult males were also recorded, but without the presence of its emitter at the surface, it was not possible to attribute them to an individual with this protocol. This lack of adult males led to large uncertainty on some parameters of the model, and mostly the value of IPI_{∞} . Both male-fitted models predict a value of IPI_{∞} that is close to 4 ms. The fact that the model fitted on juvenile males does not extrapolate to a correct adult IPI might be an indication of the second period of fast growth reported by Best²² and Ohsumi²⁴. This growth is not represented in our data, since only one male data point is at an age of 11 years old, with all the others being below 9 years old. If this assumption is correct, it would mean that there would not be such a large difference in size between male and female sperm whales if the males did not have a second period of fast growth.

We use the mean primiparous age to estimate the age of female sperm whales. However, it has one main issue that the first offspring could have died, or left the clan if it is a male. Mislabeling the second or third child as the first offspring would bring down the estimated age by 6 or 12 years. This issue is tackled by two points. Firstly the large standard deviation on the age estimation is large enough to encapsulate those errors, while also dealing with

model	Parameters			Predicted values				
	IPI_0 or IPI_{∞}	a	α or t_0	IPI_0	IPI_{∞}	$t_{72.7}$	t_{95}	t_{99}
G_M	1.57 ± 0.09	0.907 ± 0.109	0.180 ± 0.058	1.57 ± 0.09	3.91 ± 0.55	5.78 ± 2.32	15.8 ± 6.1	24.9 ± 6.1
V_M	4.25 ± 0.80	0.113 ± 0.053	- 3.950 ± 1.210	1.53 ± 0.67	4.25 ± 0.80	7.52 ± 7.73	22.5 ± 17.6	36.7 ± 17.6
G_F	1.61 ± 0.11	0.780 ± 0.067	0.146 ± 0.019	1.61 ± 0.11	3.53 ± 0.06	6.12 ± 1.04	18.6 ± 2.6	29.7 ± 2.6
V_F	3.54 ± 0.05	0.127 ± 0.016	- 4.310 ± 0.880	1.49 ± 0.27	3.54 ± 0.05	5.90 ± 1.64	19.2 ± 3.3	31.9 ± 3.3

Table 3. Fitting results of the IPI growth models. Models with a G are the Gompertz models (Eq. (1)) while the models with a V are the Von Bertalanffy models (Eq. (2)). The M and F at the end of the model's name indicate the sex. IPI_0 is the IPI at birth and IPI_{∞} is the asymptote of the model when t goes toward ∞ . $t_{72.7}$, t_{95} and t_{99} are the times when the sperm whale's IPI reaches 72.7%, 95% and 99% of its maximal IPI value respectively.

the lesser issue of the variability of the first pregnancy. Secondly, the growth curve is flat in the region of mature females. Varying the age of the point in this part of the curve only varies the estimated parameters by a little bit, and is already included in the uncertainty of those parameters. Thus estimating the age of mature females is only crucial when the female is close to the transition age between juvenile and adult.

Since all individuals are different, an alternative would have been to fit a separate growth curve to each individual and compare their differences afterward. It would give a more meaningful confidence interval for each individual growth model, and allow us to study the prediction interval by comparing the estimated size of each individual at each time t . In this paper, only four juvenile whales (one female and three males) were recorded for more than five years, and at most seven years, which we consider to be too few to be analyzed in that way. Nonetheless, those kinds of results along with the only method (observing birth) to obtain accurate age demonstrate the need to increase the focus on individuals, and to follow them from their birth.

As described in Sarano et al.⁴³, Irène's clan is to this date composed of two subgroups. During our study, the initially monolithic clan progressively divided into these subgroups (the 2 subgroups were seen together in 100% of the observations in 2013, and only 19% in 2022). The subgroups are mainly driven by genetics⁴³. The 2 larger half-brother juveniles Éliot and Tache blanche. Inversely the smaller male Roméo is in the other subgroup. Thus the new subgroups have a smaller inter-individual variation.

A potential source of error in our click dataset is the depth at which they were recorded, as described in the Materials section. Most of the clicks were recorded 50 cm below the surface, and some of them were at a depth of 20 m. Thus clicks are polluted with their surface echoes, causing interference in the signal. Acoustics leaks also produce similar issues. However, the variation of geometry during the recording (position and orientation of both the sperm whale and the hydrophone array held by the diver), allows us to differentiate between moving pulses and stable ones. Since the hydrophone array was not always available, consumer recording devices such as GoPro were used. They have the inconvenience of loosely compressing the audio signal in a way meant for human perception, and recorders are not meant to record underwater sounds. The artifacts introduced by the compression method made the annotation task harder. Also, the GoPro Hero 3 needed a waterproof case, which might alter the frequency answer. Nonetheless, all the pulses of a click should be changed similarly, except for the non-linear effects introduced by the compression. We suppose that this only increases the variance of the IPI measurement, but not its bias. This was confirmed by comparing annotations on segments where both the hydrophone array and a consumer recorder were present.

This paper lacks measurements of the body length. It prevented us from having a better comparison with the literature and producing a new IPI-to-length formula that would have spanned across a wider scale. The correlation between the length and IPI would also have helped to confirm both IPI and length measurements, at the limit of their difference in growth speed. Nonetheless, the development of the IPI in itself is meaningful as an insight on the development of the acoustic organs, which together form a key tool used by sperm whales to sense their environment. Since various factors affect the IPI value during the whales' growth, measuring the outputted IPI directly instead of estimating it from the head's growth leads to better accuracy. Even without a measurement to associate each measured IPI to a length, the birth size of around 4 m to the size of an adult female of around 11 m showed that the current state-of-the-art formula does not work for juveniles, since they extrapolate to negative IPI at birth. The only exception being the corrected formula Eq. (5) which for an IPI of 1.5 ms gives a length of 3.96 m. While this equation gives a matching result for 4 m, it still needs to be verified as it also gives a length of only 9 m for an IPI of 4 ms. Thus, until a new formula is found, or lengths are estimated from the video database of Mauritian sperm whales, Eq. (5) could be used to derive a length from the juvenile's IPI given in this paper. It was not attempted here as this correction (or an alternative on) should be studied more in-depth than just conveniently fitting our data before being used.

Other than the study of sperm whale length, a continuation of this study could be the combined analysis of trains of click such as social creaks or social codas, by fully annotating them. As used in this paper, the rhythmic structure of these series can help to tie multiple clicks to an individual. Inversely, the precise knowledge of the IPI values of each sperm whale can help to segregate interlaced codas and tie them to their emitter. It would allow to better understand an exchange of codas and correlate them to the behaviors that follow.

Finally, these results may provide useful knowledge for monitoring continuing changes in the demographic parameters of this species even without long-term mark-recapture studies on sperm whales in a region, or frequent stranding. Passive acoustics and conversion of small IPI to the corresponding age would help to assess the poorly known early life history and demography of this vulnerable species⁴⁵.

Materials

Field recordings

Video recording and underwater observations have been carried out on the west coast of Mauritius (Indian Ocean) for a global study led by Longitude 181 association, based in France, in the frame of a project called *Maubydick* initiated by the *Marine Megafauna Conservation Organization (MMCO)*, based in Mauritius. Permission to conduct the *Maubydick* project was granted by the Mauritius Prime Minister's Office on the 21st of February 2017. The underwater videos were taken between 0 and 40m depth, according to the respect of the official Charter for responsible approach and observation of marine mammals and the Maritime zones regulations (Conduct of Marine Scientific Research/Notice n° 57 of 2017) promulgated by the Mauritian Government. Prior to 2017, the data have been acquired through the various documentaries for the French television ("*Les Géants*", "*Maurice, Rodrigues, les perles des Mascareignes*", and "*Le clan des cachalots*"), with the permit MFDC/P &P/3/2015 granted by the Mauritian gouvernement and the Mauritius Film Development Corporation (MDMC). At first detection of a sperm whale group, the boat, a 15 m cabin cruiser designed for diving, stopped ca 100 m upstream considering the movement direction of the sperm whale group and dropped off the observers (a scuba

diver and 4 snorkellers), then it moved aside and remained ca 200 m away from the whales. This ensured both respect for the security rules and compliance with the charter for the responsible approach and observation of marine mammals. The scuba diver recorded videos and observations at a maximum depth of 40 m. Snorkelers waited for the cetaceans to swim by. If sperm whales did not move, snorkelers slowly and carefully swam towards them^{42,43}. The number of observers depended on the mission and was most of the time less than the maximal group of 5 described above. Among the snorkelers, one was holding the JASON array, one was in charge of the security, and the remaining snorkelers were there to improve the number of points of view, to assure that no information were lost outside. Divers were passive enough, that no sign of disturbance were recorded (no change of trajectory, no sign of escape), even when females sperm whales were nursing calves⁴⁶.

Instrumentation

Most of the database has been recorded with GoPro Hero 3-8 and SonyF55 (a video camera). As a goal of another study on this clan is to understand the relationship between individuals inside the family group and the dynamics of the Mauritian sperm whale population, the protocol has been reinforced via H. Glotin's SMIoT DYNI teams, with the design of a high sampling rate compact hydrophone array (called 'JASON'), in order to diarize each or their vocalizations^{47,48}. It evolved over the years, starting from 2 hydrophones in 2017, 3 in 2018, and 4 in 2019. The hydrophones were spaced at most by 60 cm. Its hydrophones are Cetacean Research C55 and C57. The sound recording device is the Qualilife sound card⁴⁹ allowing a sampling rate up to 1 MHz, 24 bits per channel, up to 5 channels in an embedded solution. While GoPro camera have been used alone, the JASON array always had a GoPro mounted on top of it.

Methods

We employed two methods to measure the IPI: manual annotation directly on the signal and an annotation interface. The whole IPI dataset was not annotated using the two methods, but an overlap exists between each method to verify that there is not a bias in one of the methods. In all methods, a highpass filter was used. Below 1.5 kHz, it removes the background noise which mainly consists of wave and boat noise, and divers breathing, leaving the signal above 1.5 kHz where the sperm whale click energy starts to appear. However, for multiple clicks, the energy below 10 kHz was blurred between the pulses in multiple clicks. Thus, 10 kHz highpass filters were used except for the spectrogram visualization where only 1.5 kHz highpass filters were used. For both methods and for each file, the annotators selected clicks spread uniformly as possible across the file, starting with the clicks with the highest energy, excluding clipped clicks. Click from codas were prioritized as they are easier to annotate. Echolocation clicks were not used as not emitted by the animals at the surface⁴. Both on and off-axis clicks were used. If there was a doubt about the IPI measurement, the click was discarded and another one was annotated if possible. Only clicks with at least 3 pulses visible were selected.

Manual IPI annotation

The manual annotation of the IPI was done using the software audacity⁵⁰ with a 10 kHz highpass filter. Clicks were annotated by experts by selecting a sample in P1 and selecting the corresponding sample in P2. Some annotations were done on P2P3 or P3P4, but P0P1 was avoided due to its variation based on the animal's orientation. For each file, around 10 clicks per annotated individual were annotated.

Interface for IPI annotation

The second method used for the annotation was based on a specialized interface we developed⁵¹ (see Supplementary Material S2). This annotation tool was developed to combine four usual visualizations of IPI: signal, spectrogram, autocorrelation, and cepstrum. On top of the tool, 20 seconds of the signal is shown, where a click can be analyzed by clicking on it. Then clicks (with their four visualizations) can be seen at the same time. The tool will show the results of the annotation on the four visualizations simultaneously to combine their cumulative information, with each visualization helping to filter out spurious pulse. Thus, the IPI value was chosen as the value that satisfied all the visualizations. In other term, while the annotation tool allows to save one value per visualization (except for the spectrogram as an alternate representation of the time signal), only one IPI value was annotated per click. Around 10 clicks were also annotated by file as for the manual IPI annotation method. If it was not possible to satisfy a visualization, another click was annotated instead. However, the prominence of the IPI was allowed to be low in one of the visualization as long as it was high enough in the others.

Click attribution and individual recognition

The click attribution has three distinct categories: juvenile, adult females, and adult males. The identification of the individual present in the video was done by experts using visual criteria such as scars, caudal shape, or other body markers which are described in Sarano et al.⁴². The categorization of clicks was only use to confirm the emitting whale, but not to determine its identity. Adult males are the easiest clicks to attribute since only one large male is present at a time and male emits only slow clicks or clicks with an IPI larger than the ones of non-adult male sperm whales and adult females. The second easiest category is juveniles. In our data set, recordings with multiple juveniles have juveniles that are always distinguishable by their size/IPI. For the female category, the task is a bit harder, as their size, hence their IPI, is similar and multiple individuals can be present simultaneously. Moreover, the GoPro field of view only covers part of the environment, which can lead to some sperm whales being heard but not seen in the video. The recording protocol made these kinds of events rare as the divers remained outside of the group and only happened when an animal swam back from the depth. For the video where the JASON array was present, the click direction of arrival (DoA) was computed using the time delay of arrival (TDoA) and was matched with the individual present in the same direction⁴⁷. For the selected clicks, the

TDoA were computed using cross correlation between the signal recorded by each hydrophone. 15 ms of signal centered on P1 of the first channel was used for the cross correlation. The TDoA were converted to DoA using the least square solution of $-\begin{pmatrix} x_1 y_1 z_1 \\ \dots \\ x_n y_n z_n \end{pmatrix} \begin{pmatrix} x \\ y \\ z \end{pmatrix} = c \begin{pmatrix} \tau_{01} \\ \dots \\ \tau_{0n} \end{pmatrix}$, where $\begin{pmatrix} x_1 y_1 z_1 \\ \dots \\ x_n y_n z_n \end{pmatrix}$ are the position of the hydrophone with hydrophone 0 at the origin, $\begin{pmatrix} x \\ y \\ z \end{pmatrix}$ is the DoA, c the speed of sound in water, and $\begin{pmatrix} \tau_{01} \\ \dots \\ \tau_{0n} \end{pmatrix}$ the TDoA between the hydrophones and hydrophone 0. Finally, knowing both the field of view and the fisheye effect of the camera provided a map between the DoA and the pixel coordinate inside the frames of a video. An example is shown in Fig. 5. For the rest of the videos, if only one animal is present, then loud enough clicks (according to the annotator) were attributed to the subject. If more than one animal was present, then only codas were annotated when a socio-sexual interaction happened in front of the camera. The attribution within the dyad⁵² (2 females in socio-sexual interaction) is then done by using the relative size of each animal and the IPI they should have according to the other measurements of the same female in another video (for the 9 annotated dyads, the minimum IPI different was 0.18 ms and the median 0.51 ms). Female-juvenile interaction were dealt with in a similar manner. Only one video was rejected due to incoherent IPI, and after further analysis, another pair of sperm whales were seen in the background showing a stronger social interaction. No video with more than two individuals interacting acoustically were used.

The author François Sarano agrees to have a picture of him uploaded along with this paper.

Age determination for each individual

All birth dates by month were known for juvenile sperm whales due to birth proofs during field sessions⁴². If the day of birth is not precise, it is assumed that the juvenile is born on the 15th of the month. For the mature female, the observation started too late to observe their birth. Their age was instead estimated using the genealogy tree of the clan, which was obtained by analyzing the mitochondrial DNA⁴³. With the genealogy tree, the first limits were set by sorting the parents and infants. The age at which sperm whales first give birth is around 13 years old³⁴, which sets a minimum age by adding it to the age of their firstborn. Another insight is the duration between two births which is around 6 years in this clan, which is similar to the population observed near Durban (east coast of South Africa)³⁰. Thus two adult sisters should also follow that pattern and have at least an age difference of 6 years. Finally, other observations of this group prior to our study also add proof an individual already existed at a certain time and had already reached adult size. This was also in concordance with visual observations, such as the number of scars, or skin decoloration.

Model fitting and statistical analysis

Since our measurements have uncertainty both in age and IPI, the orthogonal distance regression (ODR)⁵³ method was chosen to fit the models. The models were only fitted on female IPI.

The annotated IPI are grouped by measurement campaign (meaning at most one point per year per animal). While the animal would have grown a bit between the start and the end of the campaign, the campaigns were short enough (typically two weeks) for this growth to be negligible compared to the annotation error, and for the local growth curve to be flat enough for the mean point to also fall on the curve. The combination of more measurements helped increase the accuracy of the estimated IPI, and prevent the multiple recaptures of one sperm whale to bias the fitted model toward its own growth curve. For each grouping of IPI per campaign, the measurements are weighted according to the annotation quality (good = 1, middle = 0.5, and bad = 0.25), to produce a weighted mean IPI point and its weighted standard deviation. The quality of each file was based on

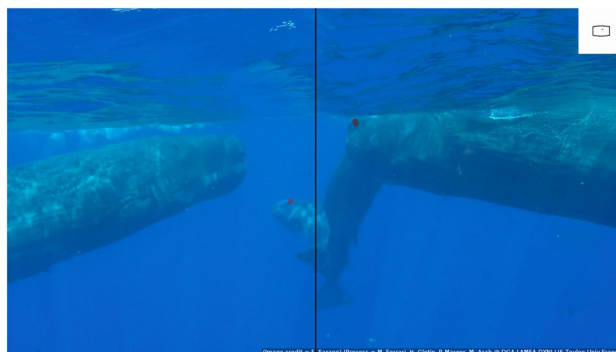


Figure 5. Frame from a GoPro video (GOPR4105.MP4) shot on the 1st of April, 2019 with different Directions of Arrival (DoA) of 3 clicks. It shows localization (red dots) of one click emitted from a male juvenile named Alexander at 3 months old, and two clicks from a male juvenile named Tache Blanche (in the foreground), 8 years old. The disambiguation between the two overlapping whales was done with the other clicks emitted when the overlap was not present. The black frame inside the white rectangle (top right) represents the field of view (FOV) of the GoPro to check the animal emitting detected clicks. Click in the white rectangle are only displayed for one frame, unlike the video where they are displayed for 7 frames.

the difficulty each annotator had to annotate clicks and is thus empirical. All IPI standard deviations have been clipped to a minimum of 0.068 ms (3 samples at 44.1 kHz). Other than increasing the variance for a series of too similar clicks, this minimum also helps with ODR which weighs each datapoint by the square inverse of the standard deviations. For the age, The standard deviation was set based on our age-determination methods. Thus, 1 day or fifteen for juveniles, and around 6 or 10 years for adults. Germines is the exception with only one year.

Thus, from the data points with their standard deviation in age and IPI, the two ODR fitted models have estimated parameters $\hat{\beta}$, along with its covariance matrix $\text{COV}(\hat{\beta})$. The covariance matrix can then be used to compute the confidence and prediction interval. The confidence interval or region⁵⁴ is the interval in which the model could be. Thus, it displays the mean growth. The prediction interval describes where a data point could be measured. It relates to inter-individual dimorphism and could be thought of as the standard deviations at a certain age. It should be noted that prediction interval has a different meaning in time series analysis, but is not used here as the goal is not to predict the future growth of a single sperm whale.

Multiple methods exist to compute the confidence interval. However, their results might vary⁵⁴. Two methods were tested. The linearized method uses the series expansion of the non-linear function:

$$f(t, \beta) = f(t, \hat{\beta}) + \nabla_{\beta} f(t, \hat{\beta}) (\beta - \hat{\beta}) + o(\beta) \quad (6)$$

From the linearized function, the standard deviation is:

$$\sigma(f(t, \beta)) = \sqrt{\nabla_{\beta} f(t, \hat{\beta})^{\text{T}} \text{COV}(\hat{\beta}) \nabla_{\beta} f(t, \hat{\beta})} \quad (7)$$

The other method is to estimate $\sigma(f(t, \beta))$ using a Monte-Carlo estimation by varying the random variable β .

Both methods agreed on the linear part of the function (before 8 y.o. and after 20 y.o.), but disagree on the non-linear part. We chose to use the Monte Carlo estimate since it produces a larger standard deviation. The confidence interval is then taken following the t-distribution. The prediction interval is built by estimating the standard deviation σ_p of the error between a new prediction and the mean growth. It should take into account all sources of variability, which in our case is the model variability $\sigma(f(t, \beta))$, the uncertainty in our data points in both directions σ_{IPI} and $\sigma_{f(t)} = \nabla_t f(t, \hat{\beta}) \sigma_t$, and finally the residual error which is the error between the mean growth and the measured IPI. Since our dataset is limited, we assumed that the residual error is independent of time.

$$\sigma_p = \sqrt{\sigma(f(t, \beta))^2 + \sigma_e^2 + \sigma_{IPI}^2 + \sigma_{f(t)}^2} \quad (8)$$

The prediction interval is then also extracted from the t-distribution.

Data availability

The dataset of sperm whale clicks used in this study is fully available at <https://cian.lis-lab.fr/ipi>. The python script used for the annotation in this study is available on the GitLab repository at https://gitlab.lis-lab.fr/maxen.ce.ferrari/ipi_annot.

Received: 16 February 2023; Accepted: 1 January 2024

Published online: 09 August 2024

References

1. Würsig, B., Perrin, W. F. & Thewissen, J. *Encyclopedia of Marine Mammals* (Academic Press, 2009).
2. Gaskin, D. *The Ecology of Whales and Dolphins* (Heinemann, 1984).
3. Shultz, S. & Dunbar, R. Encephalization is not a universal macroevolutionary phenomenon in mammals but is associated with sociality. *Proc. Natl. Acad. Sci.* **107**, 21582–21586 (2010).
4. Madsen, P. *et al.* Sperm whale sound production studied with ultrasound time/depth-recording tags. *J. Exp. Biol.* **205**, 1899–1906 (2002).
5. Backus, R. H. & Schevill, W. E. Physeter clicks. *Whales, dolphins, and porpoises* 510–527 (1966).
6. Glezer, I. *et al.* Chemical neuroanatomy of the inferior colliculus in brains of echolocating and nonecholocating mammals: Immunocytochemical study. In *Echolocation in Bats and Dolphins* 161–172 (University of Chicago Press, 2004).
7. Serio, C. *et al.* Macroevolution of toothed whales exceptional relative brain size. *Evol. Biol.* **46**, 332–342 (2019).
8. Beckman, D. *Marine Environmental Biology and Conservation* (Jones & Bartlett Publishers, 2012).
9. Ferrari, M. Study of a biosonar based on the modeling of a complete chain of emission-propagation-reception with validation on sperm whales. (Ph.D. thesis, 2020).
10. Goold, J. Behavioural and acoustic observations of sperm whales in Scapa Flow. *J. Mar. Biol. Assoc. U. K.* **79**, 541–550 (1999).
11. Rendell, L. & Whitehead, H. Vocal clans in sperm whales (*Physeter macrocephalus*). *Proc. R. Soc. Lond.* **270**, 225–231 (2003).
12. Gordon, J. C. D. The behaviour and ecology of sperm whales off Sri Lanka. Ph.D. thesis, University of Cambridge (1987).
13. Watkins, W. A. & Schevill, W. E. Sperm whale codas. *J. Acoust. Soc. Am.* **62**, 1485–1490 (1977).
14. Madsen, P., Wahlberg, M. & Möhl, B. Male sperm whale (*Physeter macrocephalus*) acoustics in a high-latitude habitat: Implications for echolocation and communication. *Behav. Ecol. Sociobiol.* **53**, 31–41 (2002).
15. Möhl, B., Wahlberg, M., Madsen, P., Heerfordt, A. & Lund, A. The nonpulsed nature of sperm whale clicks. *J. Acoust. Soc. Am.* **114**, 1143–1154 (2003).
16. Norris, K. & Harvey, G. A theory for the function of the spermaceti organ of the sperm whale. *Anim. Orientat. Navig.* 393–417 (1972).
17. Rendell, L. & Whitehead, H. Do sperm whales share coda vocalizations? Insights into coda usage from acoustic size measurements. *Anim. Behav.* **67**, 865–874 (2004).
18. Rhinelander, M. Q. & Dawson, S. M. Measuring sperm whales from their clicks: Stability of interpulse intervals and validation that they indicate whale length. *J. Acoust. Soc. Am.* **115**, 1826–1831 (2004).

19. Böttcher, A., Gero, S., Beedholm, K., Whitehead, H. & Madsen, P. T. Variability of the inter-pulse interval in sperm whale clicks with implications for size estimation and individual identification. *J. Acoust. Soc. Am.* **144**, 365–374 (2018).
20. Zimmer, W., Madsen, P., Teloni, V., Johnson, M. & Tyack, P. Off-axis effects on the multipulse structure of sperm whale usual clicks with implications for sound production. *J. Acoust. Soc. Am.* **118**, 3337–3345 (2005).
21. Berzin, A. Rate of growth of sperm whale in the north-western pacific. *Trudy Vsesoyuznogo Nauchno-Issledovatel Institut Mordovskogo Rybnogo Khozyaistva i Okeanografii* **53**, 271–275 (1964).
22. Best, P. The sperm whale off the west coast of South Africa. 5. Age, growth, and mortality. *Investl. Rep. Fish. Mar. Biol. Surv. Div.* 1–27 (1970).
23. Gambell, R. Sperm whales off Durban. *Discov. Rep.* **35**, 199–358 (1972).
24. Ohsumi, S. Age-length key of the male sperm whale in the North Pacific and comparisons of growth curves. *Rep. Int. Whal. Comm.* **27**, 295–300 (1977).
25. Evans, K. & Hindell, M. A. The age structure and growth of female sperm whales (*Physeter macrocephalus*) in southern Australian waters. *J. Zool.* **263**, 237–250 (2004).
26. Nishiwaki, M., Ohsumi, S. & Hibiya, T. Age study of sperm whale based on reading of tooth laminations, *Whales Res. Inst. Tokyo.* (1958).
27. Nishiwaki, M., Ohsumi, S. & Maeda, Y. Change of form in the sperm whale accompanied with growth. *Whales Res. Inst. Tokyo* **17**, 1–17 (1963).
28. Evans, K. & Robertson, K. A note on the preparation of sperm whale (*Physeter macrocephalus*) teeth for age determination. *J. Cetac. Res. Manag.* **3**, 101–107 (2001).
29. Hamilton, V., Evans, K., Raymond, B. & Hindell, M. A. Environmental influences on tooth growth in sperm whales from southern Australia. *J. Exp. Mar. Biol. Ecol.* **446**, 236–244 (2013).
30. Best, P., Canham, P. & Macleod, N. Patterns of reproduction in sperm whales, *Physeter macrocephalus*. *Rep. Int. Whal. Comm.* **6**, 51–79 (1984).
31. Laws, R. M. *et al.* Growth and sexual maturity in aquatic mammals. *Nature* **178**, 193–194 (1956).
32. Laird, A., Tyler, S. & Barton, A. The dynamics of growth. *Research/Development* **20**, 28–31 (1969).
33. Von Bertalanffy, L. A quantitative theory of organic growth (inquiries on growth laws. II). *Hum. Biol.* **10**, 181–213 (1938).
34. Bannister, J. The biology and status of the sperm whales off western Australia—an extended summary of results of recent work. *Rep. Int. Whal. Comm.* **19**, 70–76 (1969).
35. Miller, B. S., Growcott, A., Slooten, E. & Dawson, S. M. Acoustically derived growth rates of sperm whales (*Physeter macrocephalus*) in Kaikoura, New Zealand. *J. Acoust. Soc. Am.* **134**, 2438–2445 (2013).
36. Gordon, J. Evaluation of a method for determining the length of sperm whales (*Physeter catodon*) from their vocalizations. *J. Zool.* **2**, 301–314 (1991).
37. Growcott, A. Measuring body length of male sperm whales from their clicks: The relationship between inter-pulse intervals and photogrammetrically measured lengths. *J. Acoust. Soc. Am.* **130**, 568–573 (2011).
38. Tønnesen, P., Gero, S., Ladegaard, M., Johnson, M. & Madsen, P. T. First-year sperm whale calves echolocate and perform long, deep dives. *Behav. Ecol. Sociobiol.* **72**, 1–15 (2018).
39. Möhl, B., Larsen, E. & Amundin, M. Sperm whale size determination: Outlines of an acoustic approach. *Mamm. Seas: Gen. Pap. Large Cetaceans* **3**, 327–331 (1981).
40. Flewelling, C. & Morris, R. Sound velocity measurements on samples from the spermaceti organ of the sperm whale (*physeter catodon*). *Deep-Sea Res.* **25**, 269–277 (1978).
41. Goold, J. C., Bennell, J. D. & Jones, S. E. Sound velocity measurements in spermaceti oil under the combined influences of temperature and pressure. *Deep Sea Res. Part I* **43**, 961–969 (1996).
42. Sarano, V. *et al.* Underwater photo-identification of sperm whales (*physeter macrocephalus*) off Mauritius. *Mar. Biol. Res.* **18**, 131–146 (2022).
43. Sarano, F. *et al.* Kin relationships in cultural species of the marine realm: Case study of a matrilineal social group of sperm whales off Mauritius island, Indian Ocean. *R. Soc. Open Sci.* **8**, 201794 (2021).
44. Clarke, R., Paliza, O. & Van Waerebeek, K. Sperm whales of the Southeast Pacific. Part VII. Reproduction and growth in the female. *Lat. Am. J. Aquat. Mamm.* **9**, 8–39 (2011).
45. Taylor, B. *et al.* *Physeter macrocephalus* (amended version of 2008 assessment). *IUCN Red List Threatened Species* **2019**, e-T41755A160983555 (2019).
46. Sarano, F. *et al.* Nursing behavior in sperm whales (*Physeter macrocephalus*). *Anim. Behav. Cognit.* **10**, 105–131 (2023).
47. Ferrari, M. *et al.* 3D diarization of a sperm whale click cocktail party by an ultra high sampling rate portable hydrophone array for assessing individual cetacean growth curves. 3239–3243, In *Forum Acusticum* (2020).
48. Ferrari, M. *et al.* High-frequency near-field *Physeter macrocephalus* monitoring by stereo-autoencoder and 3d model of sonar organ. In *IEEE OCEANS* 1–4 (2019).
49. Barchasz, V., Gies, V., Marzetti, S. & Glotin, H. A novel low-power high speed accurate and precise daq with embedded artificial intelligence for long term biodiversity survey. In *Proceedings of the Acustica Symposium* (2020).
50. Audacity (2014).
51. Poupard, M., Ferrari, M., Best, P. & Glotin, H. Passive acoustic monitoring of sperm whales and anthropogenic noise using stereophonic recordings in the Mediterranean Sea, North West Pelagos Sanctuary. *Sci. Rep.* **12**, 2007 (2022).
52. Sarano, F. *et al.* A focal animal 6-points likert scale to rate intra-unit interactions in sperm whales (*Physeter macrocephalus*) off Mauritius Island. In *World Marine Mammal Conference*, 112 (2019).
53. Boggs, P. T. & Rogers, J. E. Orthogonal distance regression. *Contemp. Math.* **112**, 183–194 (1990).
54. Boggs, P. T. & Boggs, P. T. *The computation and use of the asymptotic covariance matrix for measurement error models*, US Department of Commerce, National Institute of Standards and Technology (1989).

Acknowledgements

This study was carried out under the framework of the Mauritius Maritime Zones (conduct of marine scientific research) Regulations 2017. We thank the authority of Mauritius who facilitated the Maubydick and La Voix des Cachalots program, in particular the Prime Minister Office of the Republic of Mauritius, the department for Continental Shelf, Maritime Zones Administration and Exploration (CSMZAE, Dr. Réza Badal and his team), the Albion Fisheries Research Center (AFRC; Chief Scientific officer Mr. Satish Kadhun), the Mauritius Film Development Corporation (MFDC; Mr. Sachin Jootun and Miss Eliana Timol) and the Tourism Authority (TA; Miss Khoudijah Boodoo, Director). Thanks to Longitude 181, René Heuzey from Label Bleu productions and Axel Preud'homme for providing incredible field data and observations. This study was done under the official authorization of the Mauritius Administration. We thank SMIoT Scientific Microsystem and IoT tech. dpt., in particular V. Gies and V. Barchasz for their help in the JASON device. Fieldwork, video recording, and part of the data analysis were granted by the NGOs Longitude 181 (Valence, France). Fieldwork and video recording was

also done along with some labeling by ‘Un Océan de Vie’ and ‘Label Bleu’ Film Production (Marseille, France). We thank Navin Boodhonnee for his valuable participation in the fieldwork.

Hervé Glotin is PI of the AI Chair ADSIL that he received from tANR-20-CHIA-0014 Agence Nationale de la Recherche (ANR) and DGA innovation Defense, towards deep learning for bioacoustics. He received the grants ULPCochlea ANR-21-CE04-0020, and SYLVANIA ANR-21-CE04-0019, from ANR, towards hardware and software for detection, analysis and localisation of bioacoustical signals also used in this research. He is PI of the BIODIVERSA EUROPAM 2023-2026 project on megafauna surveys by bioacoustics. These grants financed some salaries, parts of missions and material, and computers to run experiments.

Author contributions

H.G., F.S., V.S., and M.F. planned the research and designed the protocol. H.G., M.F. designed and planned the recordings with JASON. F.S., V.S., R.H. and A.P. recorded video of the sperm whales. M.F. and M.T. with H.G. did the interface of the click detector. M.T., P.G., M.F., F.S., and V.S. did the IPI annotations. M.F., P.G., H.G., F.S., and V.S. and M.T. analyzed the results. M.F. with others authors. wrote the main manuscript text. All authors reviewed the manuscript.

Competing interests

The authors declare no competing interests.

Additional information

Supplementary Information The online version contains supplementary material available at <https://doi.org/10.1038/s41598-024-51194-5>.

Correspondence and requests for materials should be addressed to M.F., F.S., V.S., P.G. or H.G.

Reprints and permissions information is available at www.nature.com/reprints.

Publisher's note Springer Nature remains neutral with regard to jurisdictional claims in published maps and institutional affiliations.



Open Access This article is licensed under a Creative Commons Attribution-NonCommercial-NoDerivatives 4.0 International License, which permits any non-commercial use, sharing, distribution and reproduction in any medium or format, as long as you give appropriate credit to the original author(s) and the source, provide a link to the Creative Commons licence, and indicate if you modified the licensed material. You do not have permission under this licence to share adapted material derived from this article or parts of it. The images or other third party material in this article are included in the article's Creative Commons licence, unless indicated otherwise in a credit line to the material. If material is not included in the article's Creative Commons licence and your intended use is not permitted by statutory regulation or exceeds the permitted use, you will need to obtain permission directly from the copyright holder. To view a copy of this licence, visit <http://creativecommons.org/licenses/by-nc-nd/4.0/>.

© The Author(s) 2024